Infrared fundamentals and phase transitions in CO_2 up to 50 GPa

Ren Lu
Bayerishes Geoinstitut, Universität Bayreuth, D-95440 Bayreuth, Germany

A. M. Hofmeister
Department of Earth and Planetary Sciences, Washington University, St. Louis, Missouri 63130
(Received 21 February 1995; revised manuscript received 10 April 1995)

Midinfrared (IR) fundamental modes of CO_2 were measured at hydrostatic pressures up to 50 GPa and room temperature. A distinct splitting in the fundamental stretching ν_3 and bending ν_2 modes marks the structural transition from phase I to III. No other solid-solid phase transitions were observed but the spectrum acquired near 2 GPa suggests that liquid CO_2 may be stable over a narrow pressure range. The number of stretching and bending modes observed for the high-pressure polymorph corroborates a *Cmca* structure. Overtone-combination modes were also observed and their frequencies agree well with previous data. The measured frequencies of overtone-combination modes and those calculated from observations of the fundamentals differ by as much as 70 cm^{-1}, which indicates a significant amount of anharmonicity for crystalline CO_2. The phase transition is not easily detected in the overtones because both phases I and III were observed between 9 and 13 GPa, and because the coexistence of two phases with overlapping bands causes the frequency of the overtone to be "curved" near the transition rather than "kinked," as was seen for the fundamentals. The sluggish kinetics and different sampling scales could explain discrepancies in transition pressure among previous studies and suggestions of structures in addition to *Cmca* and *Pa*3.

INTRODUCTION

Knowledge of the high-pressure behavior of CO_2 is crucial for understanding planetary evolution and fundamental physics of molecular crystals. Previous studies suggested that solid CO_2 undergoes a structural change from the dry-ice cubic phase, phase I, to a new structure, phase III, at pressures above $\sim$12 GPa. The reported transition pressure ranged from 11 to 18 GPa upon compression and was several GPa lower during decompression in the various x-ray and Raman experiments.[1–4] The variance in transition pressures has been attributed to hysteresis. The structure of this high-pressure phase has been controversial. Recent free-energy calculations (e.g., Ref. 5) and a subsequent x-ray crystallographic study[4] suggest an orthorhombic structure (*Cmcm*) for the high-pressure phase, but the tetragonal structure adopted by γ-N_2 is also possible. Another structure (designated as phase II) has also been proposed to exist at 0.5–2.3 GPa and room temperature[6] based on changes in both optical properties and x-ray-diffraction lines. However, neither could its structure be determined due to the limited x-ray data,[6] nor has this phase transition been detected in subsequent spectroscopic studies.[1–3]

The fundamental IR modes of solid CO_2 at high pressure have not heretofore been observed because the extremely strong absorptions lead to saturation even for the minute amount of sample in a diamond-anvil cell. Consequently, the existing high-pressure IR data consist exclusively of overtone-combination modes[1,3] which are significantly less intense. The overtone-combination mode frequencies appear to change smoothly across the transition between phase I and III. The pressure dependencies of the fundamentals are inferred and discrepancies exist amount the inferred values.[3,7]

This study presents direct observations of the mid-IR active fundamentals as well as of overtone-combination modes of CO_2 at hydrostatic pressures up to 50 GPa, which is more than double the maximum pressures previously attained. The measured fundamental frequencies differ dramatically from those inferred due to anharmonicity. The pressure-induced structural transition between phases I and III are manifest in an abrupt splitting of one fundamental mode, and in shifts in frequencies and differences in slopes ($\partial\nu/\partial P$). At low pressure ($\sim$2 GPa) our data imply that CO_2 condenses as a liquid.

SYMMETRY ANALYSIS AND 1 ATM OBSERVATIONS

CO_2 in the gaseous state possesses three internal vibrations: an asymmetric stretch ν_3 at 2350 cm^{-1} (IR active), a symmetric stretch ν_1 at 1337 cm^{-1} (Raman active), and a doubly degenerate bending ν_2 mode at 667 cm^{-1} (IR active). The Raman spectrum is complicated by Fermi resonance of $2\nu_2$ with ν_1.

Phase I, the structure assumed by CO_2 upon freezing at ambient pressure or upon compression at ambient temperature is cubic, having a $Pa3$ (T_h^6) space group.[8,9] Its 33 optically active modes consist of various splittings of the internal modes of the CO_2 molecule, rotations and/or librations R of CO_2, and translations T of CO_2 (Table I). At liquid N_2 temperatures, the frequencies of phase I are ν_3=2345 cm^{-1}, ν_1=1332 cm^{-1}, and ν_2=660 cm^{-1} (Ref. 10). These frequencies change negligibly with temperature[11] ($<1\%$) from 10 to 150 K.

Above about 12 GPa, CO_2 transforms to another structure, phase III.[1] Recent crystallographic studies indicate the *Cmca* space group,[4] which has 15 vibrations (Table I), owing to the smaller Bravais cell. It is possible that other structures exist. In particular, a tetragonal structure (the γ-N_2 phase with space group $P4_2/mnm$, Ref. 14) assumed by N_2 during compression has been proposed[3] for phase III of CO_2, although not confirmed. Theoretical free-energy calculations[15] are also compatible with this tetragonal structure. Its symmetry analysis is also included in Table I. It is clear that the number and symmetry of the internal modes present in the IR-active symmetries for each of the above crystalline structures differ: thus, structural phase transformations should be apparent in the mid-IR region.

EXPERIMENT

Gases of CO_2 and argon were condensed at liquid-nitrogen temperature into a Mao-Bell-type diamond-anvil cell (DAC) with type-II diamonds ($\frac{1}{3}$ carat) with flat-tip, 0.6 mm cutlets. Argon served as both an IR-transparent, essentially hydrostatic pressure medium and a dilutant to reduce the intensity of IR absorptions in CO_2. An all-reflecting beam condenser was used to interface the DAC with the spectrometer. Pressure was measured with the ruby fluorescence technique.[16–18] Detailed descriptions of experimental procedures are given previously.[19] Selective pressure measurements of ruby grains at the edge, center and intermediate points over the gasket hole showed essentially no differences below ~15 GPa. Above this pressure, a pressure gradient of up to about 5% was observed.

Infrared spectra were acquired using an evacuated Bomem DA3.02 Fourier transform interferometer at 1 cm^{-1} resolution above 450 cm^{-1} with a KBr beam splitter and a liquid-nitrogen-cooled HgCdTe detector.[19] All spectra were collected at room temperature with a large number of scans (3000 to 6000) for a high signal-to-noise ratio.

RESULTS

The fundamental bending ν_2 [Figs. 1(a) and 1(b)] and stretching ν_3 [Figs. 1(c) and 1(d)] vibrations of solid CO_2 are on scale at all pressures, allowing direct and precise determination of mode frequencies (Table II). Spectra below ~13 GPa have sharp and well-resolved bands whereas those above ~13 GPa (from both compression and decompression) appear much broader. All spectra acquired above pressures of 4 GPa correspond to solid CO_2 because they all show factor group splittings. The moderately intense combination mode ($\nu_1+\nu_3$) was traced to 50 GPa in both compression and decompression spectra, whereas the weaker overtone combination ($2\nu_2+\nu_3$) was resolved up to ~15 GPa in decompression spectra [Fig. 1(e) and Table II]. Only the low-pressure data is shown for ($\nu_1+\nu_3$). Spectra of the overtones at higher pressures (not shown) resemble that of the 12.8 GPa spectrum.

The spectrum taken at 2 GPa differs from all others, possessing simple, symmetrical peaks [Figs. 1(b) and 1(d)]. The frequencies clearly deviate from the trend followed at higher pressures [Figs. 2(a) and 2(b) and Table II]. Because factor-group splittings in ν_2 expected for solid CO_2 were not observed, we infer that this phase is a liquid (see discussion section).

Spectra obtained between 4.7 and 8.1 GPa from decompression [Fig. 1(b) and 1(d)] were assigned to phase I (dry ice) based on their close resemblance to the spectrum of solid CO_2 at low temperature.[10] The observed number of modes matches that expected from symmetry analysis for phase I (Table I). The stretching vibration showed a slight nonlinear dependence with pressure whereas the bending vibrations appear to depend linearly on pressure [Figs. 2(a) and 2(b)]. A ν_3 peak attributable to the isotope $^{13}CO_2$ was also observed [Fig. 1(d)]. The pressure dependence of this mode lies parallel to that of $^{12}CO_2$. Extrapolation of our data to ambient pressure gives a 1 atm pressure mode frequency of 2289.6 cm^{-1} which lies close to the observed frequency of 2283 cm^{-1}

TABLE I. Symmetry analysis of vibrational modes in structures possible for solid CO_2.

$Pa3=T_h^6$								
Γ_{optic}[a,b]	A_g (R)		E_g (R)	$3T_g$ (R)	$2A_u$	$2E_u$	$5T_u$ (IR)	
Internal modes		ν_1		ν_1	ν_3	ν_2		$\nu_3+2\nu_2$
External modes		R		$2R$	T	T	$2T$	
$Cmca=D_{2h}^{18}$								
Γ_{optic}[a]	$2A_g$ (R)	B_{1g} (R)	B_{2g} (R)	$2B_{3g}$ (R)	$2A_u$	$3B_{1u}$ (IR)	$3B_{2u}$ (IR)	B_{3u} (IR)
Internal modes	ν_1			ν_1	ν_2	$\nu_3+\nu_2$	$\nu_3+\nu_2$	ν_2
External modes	R	R	R	R	T	T	T	
$P4_2/mnm=D_{4h}^{14}$								
Γ_{optic}[a,c]	A_{1g} (R)	A_{2g}	B_{1g} (R)	B_{2g} (R)	E_g (R)	A_{2u} (IR)	$2B_{1u}$	$3E_u$ (IR)
Internal modes	ν_1			ν_1		ν_3	ν_3	$2\nu_2$
External modes		R	R		R		T	T

[a]Acoustic modes are not included. R, Raman active; IR, infrared active. See text for other abbreviations.

[b]See also Powell *et al.* (Ref. 12).

[c]A partial analysis is given by Freiman (Ref. 13).

for the isotropic peak of phase I at low temperature.[10,11]

Spectra taken at pressures above 13 GPa differ significantly from spectra acquired from phase I and thus were attributed to phase III [Figs. 1(a)–1(d)]. Differences include an increase in the number of peaks, overall broader bands, and lower intensities. Spectra obtained between 13 and 50 GPa exhibit two distinct stretching modes and three bending modes in agreement with the symmetry analysis for a *Cmca* space group (Table I). All phase III mode frequencies linearly depend on pressure [Figs. 2(a) and 2(b)], and data from compression and decompression cycles agree well. Compression spectra appear noisier at low pressures probably because the sample was initially not fully compacted. A slight deviation from the linear trend between 20 and 30 GPa [Figs. 2(a) and 2(b)] is likely to be associated with structural adjustments and local stress evidenced by the relatively high-pressure gradient in phase III. The higher fluctuation in mode frequencies of phase III is also associated with difficulties in precisely locating the maximum for the broader bands of this phase.

Features of phases I and III are both present in spectra between 8.1 and 12.8 GPa, indicating partial transformation. The proportion of phase III increases with pressure: the spectrum at 8.1 GPa appear to be mostly phase I with only a trace amount of phase III [Fig. 1(b) and 1(d)]; whereas the spectrum at 9.6 GPa shows roughly equal amounts of phase I and III, and spectrum at 12.8 GPa is nearly all phase III. Mode frequencies within this mixed-phase region are less accurately established due to overlapping peaks. As a result, the mixed-phase region deviates from the trends established for the single phase regions [Figs. 2(a) and 2(b)]. Coexistence of two phases for alkali halides over a range of pressures has also been observed and the lattice constants determined from experiments with two phases are similarly disturbed from data acquired from a uniformly transformed sample.[20] Thus, frequencies from the two-phase region were not used in the least-square fits.

Neither discontinuous behavior nor phase transitions were observed at higher pressures (up to 50 GPa). In particular, transition to another solid (e.g., phase II) (Ref. 6) is not supported by our data.

Frequencies of overtone-combination modes $(\nu_1+\nu_3)$ and $(2\nu_2+\nu_3)$ (Fig. 3) are in good agreement with previous experiments.[3,7,10] The slightly higher frequencies previously observed for the more intense $(\nu_1+\nu_3)$ mode may be due to (1) mixing with phase III or (2) the presence of LO (longitudinal optical) components in the thicker samples used in previous studies. The present study of a very dilute (thin) sample should basically consist of TO (transverse optical) component. The weaker bands of CO_2 related to isotopes of ^{13}C and ^{18}O in the

TABLE II. IR Frequencies of CO_2 as function of pressure. Frequencies are in cm^{-1}.

P(GPa)	ν_2(a)	ν_2(b)	ν_2(c)	ν_3(a)	ν_3(b)	$\nu_1+\nu_3$	$2\nu_2+\nu_3$
			Phase III (compression data)				
20.2	652.8			2368.4	2439.8	3809.2	
22.5	652.2	636.1		2374.9	2448.6	3822.6	
25.3	651.0	636.7		2378.8	2456.6	3832.4	
28.6	650.2	636.5		2384.8	2460.0	3839.7	
32.3	649.0	638.2		2387.8	2467.1	3846.4	
36.6	649.2	638.4	624.3	2395.5	2477.9	3861.1	
43.2	648.6	637.6	618.2	2409.2	2499.7	3881.2	
46.7	648.9	637.3	616.3	2413.8	2506.6	3892.2	
50.4	649.1	639.0	611.0	2419.8	2515.1	3898.7	
			Phase III (decompression data)				
50.4	649.1	639.0	611.0	2515.7	2419.8		
44.3	648.9	640.7	618.2	2499.7	2410.4		
38.2	649.5	640.6	624.8	2480.4	2395.9		
29.8	648.9	639.9	629.1	2461.7	2381.4		
19.5	651.8	639.6		2438.1	2361.7		
12.8	653.7	640.4		2416.2	2349.0	3778.4	3638.2
9.6	653.6	639.5		2405.7	2342.0	3766.4	3631.4
8.1					2344.2		
			Phase I (decompression data)				
12.8	659.6						
9.6	660.6	643.7		2393.6			
8.1	658.5	644.8		2388.1		3760.8	3627.9
6.0	659.0	646.9		2381.0		3751.0	3623.2
4.7	659.7	648.7		2374.4		3742.2	3619.7
			Liquid (decompression data)				
2.0	663.4			2345.9		3709.8	3605.7

$(\nu_1+\nu_3)$ region[10] are not observed due to use of the thin sample.

In contrast to the behavior of the fundamentals, no discontinuities were observed in the frequencies of the overtone-combination modes (Fig. 3). A single quadratic curve could represent all the observed data. The phase I to III transition only induced minor changes in intensity and shape of the overtones, such that overtones for phase I are slightly asymmetric in shape and have a narrower half-width as compared to those of phase III [Fig. 1(e)].

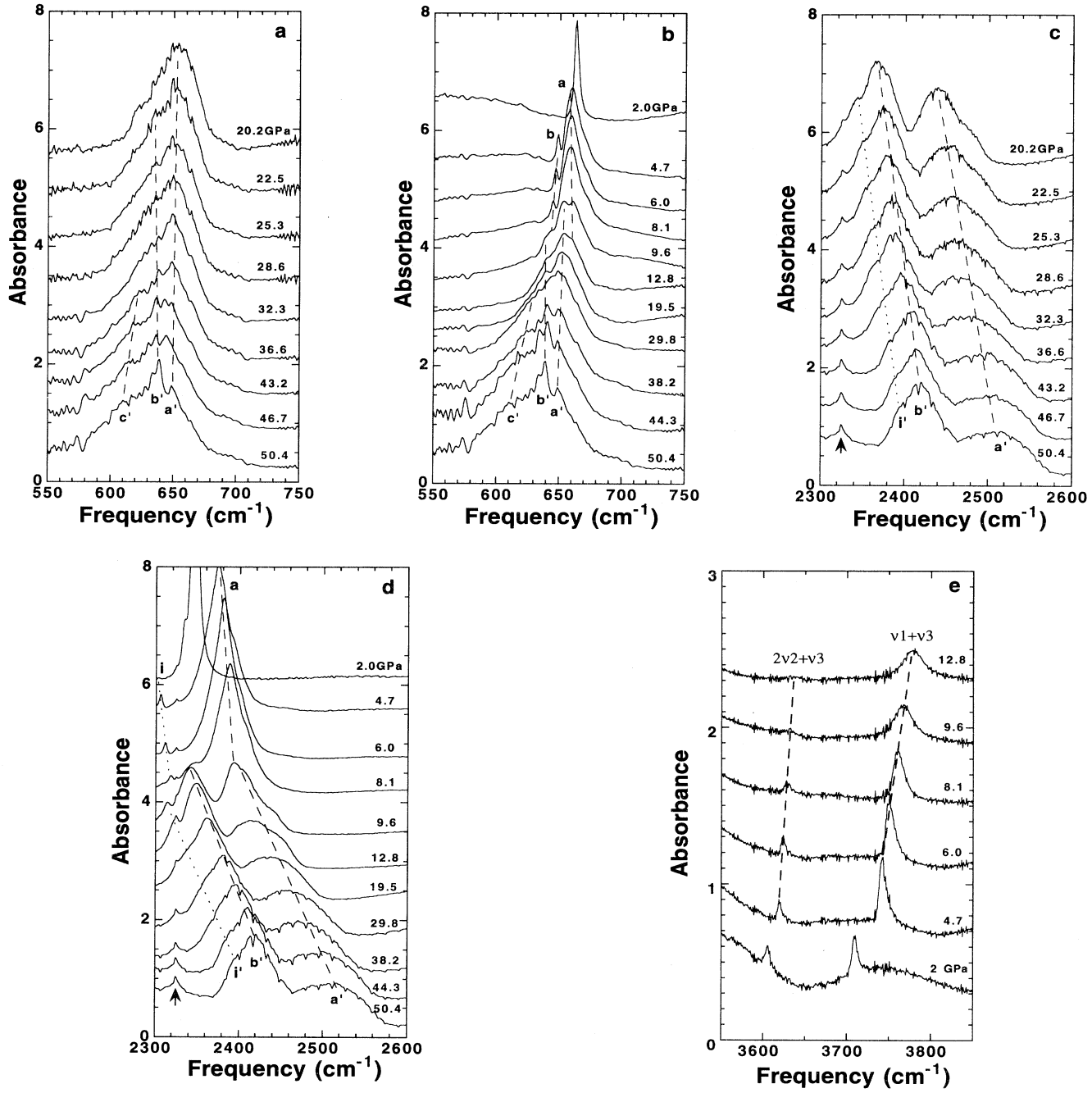

FIG. 1. IR spectra of CO_2 at high pressures. (a) Bending vibrations of phase III during compression. (b) Bending vibrations during decompression. (c) Stretching vibrations of phase III during compression. (d) Stretching vibrations during decompression. (e) The overtone-combination region during decompression. Modes from phase III are labeled by primed letters. The shoulders in the stretching region (traced by dotted lines and labeled "*i*") which are parallel to *a* and *a'* are isotopic peaks of phases I and III, respectively. The pressure-independent peak at ~ 2325 cm^{-1} present in the stretching region (indicated by an arrow) is an artifact. The interference fringes in the stretching region at high pressures are due to the size of the gasket aperture.

Fermi resonance, originating from accidental degeneracy of ν_1 with the overtone $2\nu_2$ (Ref. 21), induces a poorly resolved band consisting of an upper component ν_+ and a lower component ν_- in Raman measurements. These two components have been used to calculate ν_1 based on Fermi resonance theory (e.g., Ref. 7). The 1 atm and low-temperature results are 1347, 1348, and 1352 cm^{-1} (from Ref. 22, 7, and 23, respectively). Fermi resonance is not present in the IR overtones,[10] allowing calculation of ν_1 readily from the most intense overtone. Calculation of ν_1 from our observed pressure dependences of the combination $(\nu_1+\nu_3)$ and of ν_3 (Fig. 4) is similar to that calculated from the available high-pressure Raman data on phase I.[7] A small difference exists between the present result and those from previous studies especially near the phase I to III transition. The differences are probably related to the coexistence of the two phases over a wide pressure region, and different proportions of the phases between the experiments.

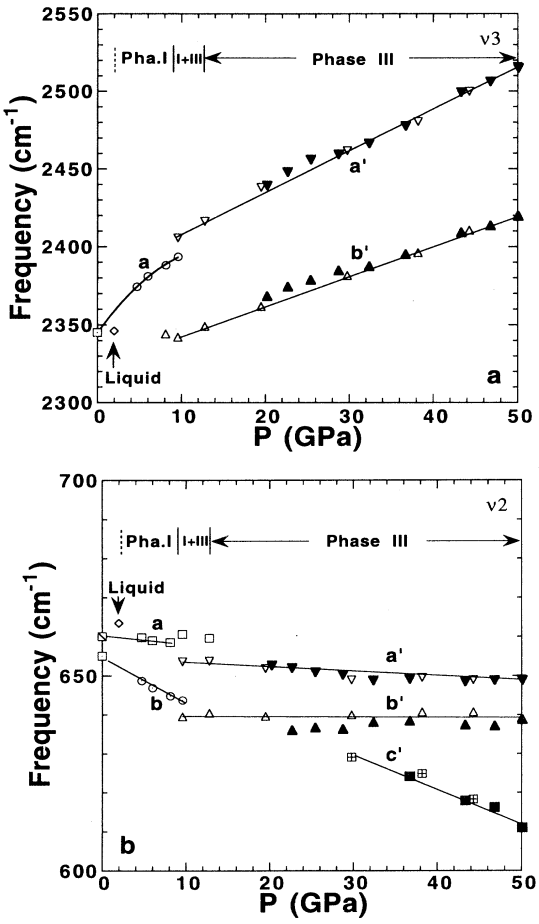

FIG. 2. Frequency of internal modes of CO_2 as function of pressure. (a) Stretching modes ν_3 and (b) bending modes ν_2 from compression (solid symbols) and decompression (open symbols). The vertical scale is highly expanded in (b). Solid lines are from least-square fits. Ambient pressure data are cryogenic measurements (Refs. 10 and 11). The data point at 2 GPa (open diamond) appears to be a liquid phase (see text).

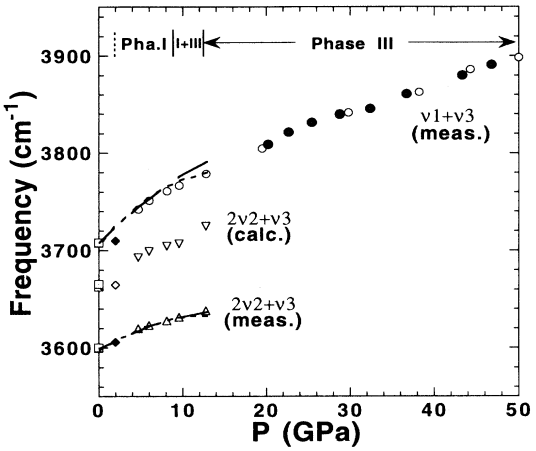

FIG. 3. Frequency of the overtone-combination modes as function of pressure. The present data (labeled "meas.") are open circles and upward-pointing triangles (from decompression) and solid circles (from compression). Downward-pointing triangles (labeled "calc") are calculated (see text). The open symbols at ambient pressure are values from low temperature (Refs. 10 and 11). Long dashed lines are previous measurements of Aoki, Yamawaki, and Sakashita (Ref. 3) and short dashed lines are those of Hanson and Jones (Ref. 7). Data points at 2 GPa of this study (solid diamonds for measurements and open diamond for the calculation) are for the liquid phase.

DISCUSSION

Phase transitions

Several linear molecules (CO_2, N_2O, and N_2) crystallize in the $Pa3$ space group at low temperature and ambient pressure. Their higher-pressure polymorphs occupy vari-

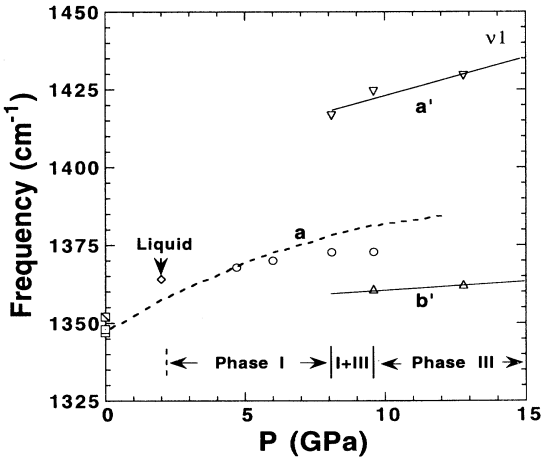

FIG. 4. Frequency of the Raman-active symmetric stretch ν_1 calculated from measurements of ν_3 and of the observed combination $(\nu_1+\nu_3)$. Data at ambient pressure are from Cahill and Leroi (Ref. 23) (slashed open square), lower value of Hanson and Jones (Ref. 7) (dotted square), and the lowest value of Anderson and Sun (Ref. 22) (open square). The least-square fit to the data of Hanson and Jones (Ref. 7) up to ~12 GPa is plotted as a dashed line.

ous structures. The β-N_2O structure[24] has the space group of *Cmca* (D_{2h}^{18}) whereas the γ-N_2 phase[14] crystallizes in the space group $P4_2/mnm$. Both of these structures have been proposed[3,15] for the high-pressure polymorph (phase III) of CO_2. These structures are related and may be visualized as follows. For the low-pressure $Pa3$ phase (the dry-ice phase), all the molecules align along body diagonals. The β-N_2O phase is obtained by rotating all molecules into the bc plane about axes perpendicular to the individual molecular axes. The γ-N_2 phase is achieved by further rotating the molecules within the bc plane so that molecules in the adjacent planes are orthogonal to each other. Sketches of these three structures have been previously presented (e.g., Refs. 13 and 24).

The significant change in symmetry for the cubic to orthorhombic phase transition should remove degeneracies and induce mode splitting (Table I). The present IR data show three ν_2 and two ν_3 bands for the high-pressure phase. Thus, the observed number of bands agrees with a *Cmca* symmetry [as deduced by Aoki *et al.*[4]] but not $P4_2/mnm$ which possesses only only ν_3 band (Table I).

In contrast to fundamental modes, frequencies of the overtone-combination modes (Aoki, Yamawaki, and Sakashita[3] and present work) do not change discontinuously with pressure at the phase transition [Figs. 1(e) and 3]. Mode frequencies of the overtones tend to be "curved" near the transition rather than "kinked," as was seen for the fundamentals. Only a minor change in mode profile is detectable across the phase I and III transition [Fig. 1(e)]. The above comparison suggests that overtone-combination modes are not sufficiently sensitive indicators for phase transitions. The indistinct separation between phase I and III in overtone-combination modes may have partially contributed to the discrepancies in the reported transition pressures.

Our spectroscopic data on fundamental modes clearly show a large overlapping region of phase I and III between 8.1 and 12.8 GPa. This extended mixed-phase region shown in our IR data reflects a large degree of hysteresis and sluggish kinetics of this phase transition.

The x-ray data[4] did not show a region where both phases overlap. Moreover, the transition pressure at room temperature suggested by the x-ray data (11.8 GPa) appears to correlate with the pressure for complete conversion from phase I to III. This difference between the present IR results and the previous crystallographic study is due to sampling scale: coherent diffraction requires some 100's of juxtaposed unit cells whereas IR spectra can be used to measure solute in a solvent. That is, IR spectroscopy is sensitive to small amounts present in a mixture but x-ray diffraction is not.

Raman spectroscopic data[1,2] do not show an overlapping region. However, the transition pressure is not consistent among the various experiments. Observation of a single phase occurs because the sampling scale in Raman experiments is much smaller than that in IR experiments and because photo stimulation in Raman experiments can accelerate phase transitions.

A phase diagram for CO_2 is constructed based on the current room-temperature data and previous low-temperature studies. The pressure of 12.8 GPa for which we observe the initiation of phase I on decompression from phase III appears to be the equilibrium phase boundary at room temperature, and the pressure of 8.1 GPa at which back transition to phase I is completed is a kinetic boundary with a ~5 GPa overstepping pressure. The transition pressure at low temperature is not yet reliably constrained because the various external modes observed in Raman experiments do not show a consistent and distinct transition pressure. Probably, the transition pressure of ~11 GPa during compression in the low-temperature Raman experiments[2] correspond to the equilibrium boundary, and the lower transition pressure from decompression may be associated with a kinetic boundary. The proposed boundary between phase I and III has a nearly vertical slope (Fig. 5).

The spectrum observed at 2 GPa suggests a liquid as evidenced by the symmetric peaks and the absence of factor-group splittings that are expected for a solid phase. This phase cannot be a gas because the peaks are too broad. The liquid phase was not seen in the Raman experiments[2] because the temperature was too low. The liquid phase was not detected by the previous IR measurements of the overtones[3,7] because these data are not sufficient to distinquish phase transitions [see Fig. 1(e)]. Regarding the crystallographic studies, Aoki *et al.*[4] did not report data at these low pressures whereas Olinger[26] observed the dry-ice phase at room temperature and between 1.04 and 10.11 GPa. It is possible that (1) the sample partially converted because an amorphous liquid phase cannot be detected by x-ray crystallography or (2) the transition has a large hysteresis loop, as was observed

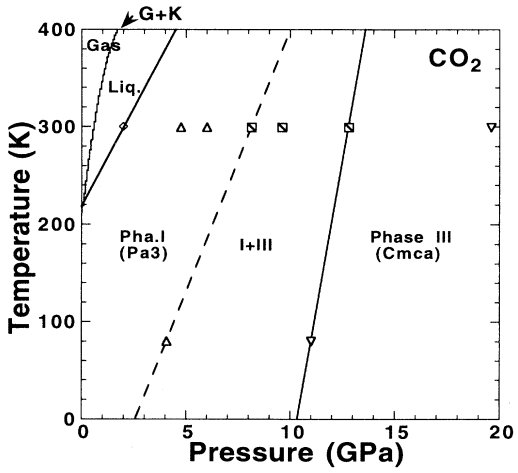

FIG. 5. Phase diagram of CO_2. The equilibrium boundary between phase I and III (long solid line) is constrained by the present data at ambient temperature and by Raman data (Ref. 2) at 80 K. Dashed lines, the kinetic phase boundary between phase I and III. The region of mixed phases I and III is indicated by slashed open squares, and phase I and III are indicated by upward and downward triangles, respectively. The liquid-to-phase I boundary (short solid line) is constrained by the present data at 2 GPa. The wiggly solid line labeled (G+K) is the phase boundary from Grace and Kennedy (Ref. 25) and is probably the gas-to-liquid transition (see text).

for the *Pa*3 to *Cmca* transition. Thus, the previous data do not rule out the existence of a liquid phase at high pressure.

Observations of a sluggish transition in CO_2 at ~ 2.2 GPa (Ref. 27) and the proposal of a transition to "phase II" at ~ 2.3 GPa (Ref. 6) are consistent with the liquid-solid transition observed in our spectra at ~ 2 GPa. Previously, Grace and Kennedy[25] concluded that the liquid to solid transition occurred at ~ 0.6 GPa. However, this "melting point" was determined from a discontinuity in the pressure-volume curve derived from a piston-cylinder experiment and, thus, was not a direct measurement of the structure. It is possible that the pressure-volume study resolved the gas-to-liquid transition because of the large volume difference between these two states.

Our observation of a solid-to-liquid transition at very high pressure may be connected with experimental conditions: our experiments were hydrostatic at this pressure with CO_2 diluted in argon. Only one previous study (Olonger[26]) definitively observed the dry-ice phase between 1 and 2 GPa. However, these experiments used CO_2 as its own pressure medium, which would not be hydrostatic, and used commercial powdered dry ice which contains a binding agent. Possibly, either the binder or the shear present caused freezing at lower pressures. Alternatively, the finely divided CO_2 in our experiments converted to liquid at a higher pressure during decompression either due to the size of the CO_2 droplets or to mixing effects with the Argon matrix. We tentatively propose that at ambient temperature, CO_2 undergoes a gas-to-liquid phase transition near 0.6 GPa whereas the liquid-to-solid (dry-ice phase) transition occurs in the vicinity of 2 GPa (Fig. 5). The precise field of stability for the liquid phase is currently being investigated.

Anharmonicity

A dramatic difference up to ~ 70 cm^{-1} is found between the observed frequency of the combination $(2\nu_2+\nu_3)$ and that calculated from measurements of the fundamentals ν_2 and ν_3 (Table II and Fig. 3). This difference appears to increase slightly with pressure. A much smaller difference (~ 15 cm^{-1}) is found between the combination $(\nu_1+\nu_3)$ and the sum of fundamentals ν_1 and ν_3. These differences reflect a large degree of anharmonicity in CO_2 crystals as these overtone-combination vibrations originate from elevated energy states (e.g., Ref. 10). The significant anharmonicity is attributed to the high dipole moment for the intramolecular vibrations ν_2 and ν_3.[28] Thus, it is expected that anharmonicity is more pronounced for the overtone combination $(2\nu_2+\nu_3)$ and less significant for the combination $(\nu_1+\nu_3)$.

The degree of anharmonicity poses a problem to deducing fundamentals solely from overtone combinations because their frequencies are not equal to the sum of the appropriate fundamentals. However, an accurate slope $(d\nu/dP)$ for the fundamental modes may be established from data on overtone combinations because the parallel curvature of fundamentals and overtone combinations (Fig. 3). Thus, fundamental frequencies may be obtained by using independent measurements of fundamental frequencies at low temperature and ambient pressure in conjunction with the slopes $(d\nu/dP)$ obtained from overtone-combination modes at high pressures.

Pressure derivatives

Stretching vibrations show pronounced positive pressure shifts whereas bending vibrations have small negative shifts in both phases I and III (Table III). The variation in slope between the two types of modes is large in phase III but not as drastic as that in phase I (Table III), presumably due to differences in compressibility. The apparent softening of the bending mode has been attributed to internal molecular anharmonicity[7] which is particularly associated with bending vibrations in CO_2 molecules.

Apparent differences exist between the present pressure derivatives of fundamental frequencies and those reported previously.[3,7] The very good agreement in directly measured modes (i.e., overtone combination, see Fig. 3)

TABLE III. Pressure derivatives and Grüneisen parameters of fundamental modes. ν_0 is in cm^{-1}, $d\nu/dP$ is in cm^{-1}/GPa and $d^2\nu/dP^2$ is in cm^{-1}/GPa^2. γ_{i0} is calculated from Eq. (1), using $K_T=2.93$ GPa (Ref. 9).

Ice I (cubic phase *Pa*3)				
Mode	ν_0	$d\nu/dP$	$d^2\nu/dP^2$	$\gamma_{i0}(\times 10^{-3})$
Bend $(\nu_2 a)$	660[a]	−0.16		−0.71
Bend $(\nu_2 b)$	655[a]	−1.29		−5.77
Asymmetric stretch (ν_3)	2345[a]	+7.43	−0.25	+9.28
Symmetric stretch (ν_1)[b]	1350[a]	+5.05	−0.28	+10.9
Ice III (orthombic phase *Cmca*)				
Bend $(\nu_2 a)$	654.2[c]	−0.12		
Bend $(\nu_2 b)$	640.3[c]	−0.09		
Bend $(\nu_2 c)$	657.1[c]	−0.89		
Asymmetric stretch $(\nu_3 a)$	2384.3[c]	+2.60		
Asymmetric stretch $(\nu_3 b)$	2335.7[c]	+1.67		

[a]For phase I, ambient pressure values were obtained from extrapolation of low-temperature data (Refs. 7 and 10) to ambient temperature.
[b]Calculated from $(\nu_1+\nu_3)$ and ν_3.
[c]For phase III, values are from linear extrapolation to ambient pressure.

indicates that the apparent difference in fundamentals is due to the method used in deducing fundamentals from overtone combinations in the previous studies. Furthermore, a thick sample such as those studied in previous experiments tends to yield higher peak positions because LO components contribute to the peak.[29] The effect is magnified by non-normal incidence in the DAC experiments.

Mode Grüneisen parameters

Mode Grüneisen parameters are calculated from

$$\gamma_{i0} = -\frac{V}{\nu_{i0}}\left[\frac{\partial \nu_i}{\partial V}\right] = \frac{K_T}{\nu_{i0}}\left[\frac{\partial \nu_i}{\partial P}\right]_0, \quad (1)$$

where V is volume, K_T is bulk modulus, and ν_i is a mode frequency. We believe it is appropriate to use an initial frequency from low temperature and ambient pressure studies because mode frequencies are almost unchanged with temperature (e.g., Refs. 2 and 11). The calculated γ_{i0}'s (Table III) show contrasting response to pressure for bending and stretching vibrations. The large positive values for stretching modes reflect a pronounced stiffening of the C-O bonds by external pressures. The slight softening of bending modes (i.e., negative values) has been related to molecular anharmonicity[7] and is not related to structural instability.

CONCLUSIONS

Internal infrared fundamental stretching and bending modes were directly measured up to 50 GPa. The transition from the dry-ice phase to the higher pressure phase was clearly shown by mode splittings. The structure of this high-pressure phase was confirmed as *Cmca*. Both phases coexist over a wide range of pressures indicating a very sluggish kinetics in this phase transition. Overtone-combination modes showed only minor changes in peak shape across the above phase transition which suggests that these modes are not sensitive indicators for phase transitions. A liquid phase was also observed at very low pressure.

ACKNOWLEDGMENTS

This work was supported by the David and Lucile Packard Foundation and NSF Grant No. EAR-9205991. We wish to thank Dr. K. Aoki (National Institute of Materials and Chemical Research, Tsukuba, Japan) for providing detailed descriptions of his published measurements. Valuable discussions with Dr. Hyunchae Cynn (UC Davis) are appreciated.

[1]R. C. Hanson, J. Phys. Chem. **89**, 4501 (1985).
[2]H. Olijnyk, H. Däufer, H. J. Jodl, and H. D. Hocheimer, J. Chem. Phys. **88**, 420 (1988).
[3]K. Aoki, H. Yamawaki, and M. Sakashita, Phys. Rev. B **48**, 9231 (1993).
[4]K. Aoki, H. Yamawaki, M. Sakashita, Y. Gotoh, and K. Takemura, Science **263**, 356 (1994).
[5]B. Kuchta and R. Etters, Phys. Rev. B **47**, 14 691 (1993).
[6]L. Liu, Nature (London) **303**, 508 (1983).
[7]R. C. Hanson and L. H. Jones, J. Chem. Phys. **75**, 1102 (1981).
[8]J. de Smedt and W. H. Keesom, Proc. R. Acad. Amsterdam, **27**, 839 (1924).
[9]L. Liu, Earth Plane Sci. Lett. **71**, 104 (1984).
[10]D. A. Dows and V. Schettino, J. Chem. Phys. **58**, 5009 (1973).
[11]S. A. Sandford and L. J. Allamandola, Astrophys. J **355**, 357 (1990).
[12]B. M. Powell, G. Dolling, L. Piseri, and P. Martel, *Symposium on Neutron Inelastic Scattering* (IAEA, Vienna, 1972), p. 207.
[13]Y. A. Freiman, Sov. J. Low. Temp. Phys. **16**, 559 (1990).
[14]A. F. Schuch and R. L. Mills, J. Chem. Phys. **52**, 6000 (1970).
[15]R. D. Etters and B. Kuchta, J. Chem. Phys. **90**, 4537 (1989).
[16]G. J. Piermarini, S. Block, J. D. Barnet, and R. A. Forman, J. Appl. Phys. **46**, 2774 (1975).
[17]A. P. Jephcoat, H. K. Mao, and P. M. Bell, in *In Hydorthermal Experimental Techniques,* edited by G. C. Ulmer and H. L. Barnes (Wiley, New York, 1987, pp. 469-506).
[18]H. K. Mao, P. M. Bell, J. W. Shaner, and D. J. Steinberg, J. Appl. Phys. **49**, 3276 (1978).
[19]R. Lu and A. M. Hofmeister, Phys. Chem. Minerals **21**, 78 (1994).
[20]N. Hamaya and S. Akimoto, High Temp. High Pressures **13**, 347 (1981).
[21]J. F. Bertran, Spectrochim. Acta **39A**, 119 (1983).
[22]A. Anderson and T. S. Sun, Chem. Phys. Lett. **8**, 537 (1971).
[23]J. E. Cahill and G. E. Leroi, J. Chem. Phys. **51**, 1324 (1969).
[24]R. L. Mills, B. Olinger, D. T. Cromer, and R. LeSar, J. Chem. Phys. **95**, 5392 (1991).
[25]J. D. Grace and G. C. Kennedy, J. Phys. Chem. Solids **28**, 977 (1967).
[26]B. Olinger, J. Chem. Phys. **77**, 6255 (1982).
[27]P. W. Bridgman, Proc. Am. Acad. Arts Sci. **72**, 207 (1938).
[28]H. Yamada and W. B. Person, J. Chem. Phys. **41**, 2478 (1964).
[29]R. G. Berreman, Phys. Rev. **130**, 2193 (1964).